LUND UNIVERSITY

Non-negative least squares fitting of multi-exponential T2 decay data: Are we able to accurately measure the fraction of myelin water?

Wiggermann, Vanessa; Vavasour, Irene M; Hernandez-Torres, Ernedino; Helms, Gunther; MacKay, Alex L; Rauscher, Alexander

Published in:
Non-negative least squares fitting of multi-exponential T2 decay data: Are we able to accurately measure the fraction of myelin water?

2019

Document Version:
Peer reviewed version (aka post-print)

Link to publication

Citation for published version (APA):
Wiggermann, V., Vavasour, I. M., Hernandez-Torres, E., Helms, G., MacKay, A. L., & Rauscher, A. (2019). Non-negative least squares fitting of multi-exponential T2 decay data: Are we able to accurately measure the fraction of myelin water? In *Non-negative least squares fitting of multi-exponential T2 decay data: Are we able to accurately measure the fraction of myelin water?* (Vol. 27). [4402] (Proc Intl Soc Magn Reson Med; Vol. 27). International Society for Magnetic Resonance in Medicine. http://indexsmart.mirasmart.com/ISMRM2019/PDFfiles/4402.html

Total number of authors:
6

LUND UNIVERSITY

PO Box 117
221 00 Lund
+46 46-222 00 00

Non-negative least squares fitting of multi-exponential T2 decay data: Are we able to accurately measure the fraction of myelin water?

Vanessa Wiggermann[1,2,3], Irene M Vavasour[3,4], Enedino Hernandez-Torres[2,3], Gunther Helms[5], Alexander L MacKay[1,3,4], and Alexander Rauscher[1,2,3,4]

[1]Physics and Astronomy, University of British Columbia, Vancouver, BC, Canada, [2]Pediatrics, University of British Columbia, Vancouver, BC, Canada, [3]UBC MRI Research Centre, University of British Columbia, Vancouver, BC, Canada, [4]Radiology, University of British Columbia, Vancouver, BC, Canada, [5]Lund University, Lund, Sweden

Synopsis

The ability to determine the myelin water fraction (MWF) in vivo is essential to assessments of neurodevelopmental myelination and myelin damage in neurodegenerative diseases. The analysis of multi-exponential T2 decay data relies on the non-negative-least-squares (NNLS) fitting, which may be sensitive to the chosen fitting parameters. We performed simulations to explore the outcomes of NNLS under different parameter selection. The lowest allowed T2 was found to have the largest effect on correctly estimating the T2 of different water pools as well as the MWF. Lower refocusing FAs led to further underestimation of the MWF.

Introduction

The ability to determine the myelin water fraction (MWF) in vivo[1] is essential to assessments of neurodevelopmental myelination and myelin damage in neurodegenerative diseases. Multi-echo spin-echo imaging has been shown to correlate with optical density measurements of myelin lipids[2,3]. However, as MW imaging has been extended to 48-echoes, applied at higher magnetic fields[3] and investigated post-mortem during fixation[4], selection of post-processing parameters for the non-negative least squares fitting (NNLS) needs to be revisited. We used simulations to explore the outcomes of NNLS fitting for different parameter selections in a given water environment at 3T and drew parallels to *in vivo* data.

Methods

Independent decay data were computed by multi-echo spin-echo simulations of the magnetization of 256x256 spins in with given T_1 and T_2-properties, taken from literature to mimic white matter values[5,6]. Various resonance frequencies were assigned to the different water compartments[7], after computing the local magnetic environment from tissue magnetic susceptibilities. All T_1's, T_2's and resonance frequencies were assigned to each spin by random sampling from a Gaussian distribution. Finally, Gaussian noise was added to the images. The voxel and its properties are shown in **Figure 1**. The MWF, i.e. the amount of MW relative to all water within a voxel, was 21%. Decay data were computed assuming a signal-to-noise ratio of 300, imperfect refocusing flip angles (FA=30,150,170,180º) and MWT_2-times (5,10,15,20 ms) using a 32-echo sequence with TE/ΔTE/TR=10/10/1000ms. Decay curves were analyzed by fitting the measured decay curve with decay curves estimated by the extended-phase-graph algorithm to estimate FA in the presence of stimulated echoes[8,9], while minimizing $\chi 2$ with respect to FA. Regularized NNLS was employed with varying numbers of T_2-components (nT_2) to fit the decay curves. The estimated parameters, i.e. the FA, the geometric mean T_2 of the intra/extracellular water (GMT2 IEW), GMT2 of the MW and the MWF were computed under varying nT_2s (20,32,40,80,120) and different T_2-ranges for which the shortest T_2 was varied ($T_{2,1}$=5-15ms, $T_{2,end}$=2s).

Results

The FA estimation was independent of nT_2. The computed FAs differed from the true FAs by 2.46±1.49, 3.00±0.51, 1.99±0.58 and 2.36±0.51 for 130,150,170,180º, respectively. **Figure 2** shows the estimated GMT_2 IEW values. As FA decreaed, the GMT_2 IEW moved further away from the reference: 69.70±0.71ms (180º), 69.74±0.62ms (170º), 68.85±1.08ms (150º), 67.93±1.38ms (130º). For MWT_2 values, lower refocusing FAs resulted in greater deviations from the true GMT_2 IEW. This was explored in more detail in **Figure 3**, by comparing the computed T_2-distributions. For all FAs, the GMT_2 of MW and IEW were well determined when $T_{2,1}$ was less than T_2 of MW. When T_2 MW was shorter than the first allowed T_2, the MW peak was incompletely described and the estimated MWT_2 depended on the value of $T_{2,1}$. However, the GMT_2 IEW was accurately estimated. Finally, we compared the estimated MWF, with respect to FA, nT_2's and $T_{2,1}$ (**Figure 4**). Again, MWFs were well estimated if $T_{2,1}$ was less than MWT_2. Note that once the MW peak was fully captured, further shortening of $T_{2,1}$ did not change the MWF. With decreasing FA, the MWF was underestimated. When assessing the impact of changed analysis parameters on in vivo data acquired at 3T with the imaging parameters matching the simulation parameters (Figure 5), we noted visually an improvement in the assessed MWF when lowering $T_{2,1}$ from 14 to 12ms. Both GMT_2 IEW and MWF were in line with the observations of the simulation, with stronger effects observed for single voxels. FAs in the regions-of-interest were 151.7,164.3,154.3º in the internal capsule, white matter and globus pallidus, respectively.

Discussion

Although the true FAs were well captured by the extended-phase-graph algorithm, MWF may be under-estimated, even when the MWT_2 was within the T_2-range. The GMT_2 of IEW and MW shortened slightly at lower FAs if $T_{2,1}$<MW T_2, but MWT_2 estimation failed if $T_{2,1}$ was chosen too long. FAs at 3T are generally greater than 150, but regions of low FA as well as further T_2-shortening at higer magnetic field strength, or due to fixation, will be problematic for estimating MWF correctly. *In vivo* data showed good correspondence with the simulations. Single-voxel data were affected by the choice of parameters, but averages within regions containing multiple voxels provided stable estimates.

Conclusions

The MWF was robustly estimated with respect to many parameters. Successfully measuring the MWF however depends on the actual MWT_2, which is unknown, and the chosen T_2-range, relative to the MWT_2. By lowering the T_2-range, the MW signal is better captured. Further work should investigate how underestimations of the MWF at lower, known FAs can be recovered.

Acknowledgements

No acknowledgement found.

References

1. MacKay A, Whittall K, Adler J, et al. In vivo visualization of myelin water in brain by magnetic resonance. Magn Reson Med 1994;31(6):673-677.

2. Laule C, Leung E, Li DKB, et al. Myelin water imaging in multiple sclerosis: quantitative correlations with histopathology. Mult Scler 2006;12(6):747-753.

3. Laule C, Kozlowski P, Leung E, et al. Myelin water imaging of multiple sclerosis at 7T: correlations with histopathology. NeuroImage 2008;40(4):1575-1580.

4. Shatil, AS, Uddin MN, Matsuda KM, et al. Quantitative Ex Vivo MRI Changes due to Progressive Formalin Fixation in Whole Human Brain Specimens: Longitudinal Characterization of Diffusion, Relaxometry, and Myelin Water Fraction Measurements at 3T. Frontiers in medicine 2018;5:31.

5. Labadie C, Lee JH, Rooney WD, et al. Myelin water mapping by spatially regularized longitudinal relaxographic imaging at high magnetic fields. Magnetic resonance in medicine 2014;71(1):375-387.

6. MacKay A, Laule C, Vavasour I et al. Insights into brain microstructure from the T2 distribution. Magnetic resonance imaging 2006;24(4):515-525.

7. Alonso-Ortiz E, Levesque IR, Pike GB. Impact of magnetic susceptibility anisotropy at 3 T and 7 T on T2*-based myelin water fraction imaging. NeuroImage 2017;182:370-378.

8. Hennig J. Multiecho imaging sequence with low refocusing flip angles. JMRI 1988;78(3):397-407.

9. Prasloski T, Mädler B, Xiang Q-S, et al. Applications of stimulated echo correction to multicomponent T2 analysis. Magn Reson Med 2012;67(6):1803-1814.

Figures

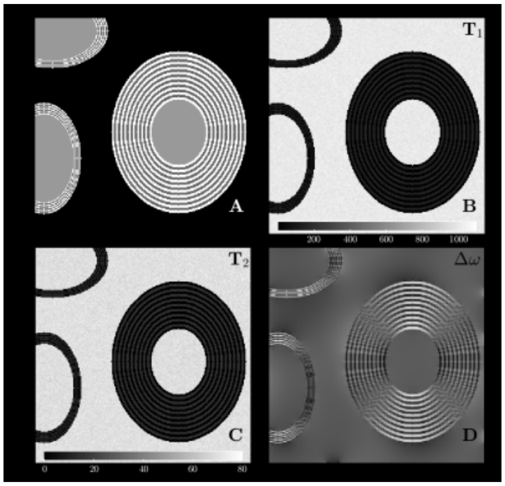

Figure 1: **Assumed 2D-voxel with different compartments of varying, compartment-specific T_1's, T_2's and resonance frequencies.** (A) shows the model voxel, in which the myelin water fraction, i.e. the fraction of water within the myelin lipid bilayers relative to all water present in the voxel was approximately 21%. (B) and (C) display the respective T_1 and T_2 of the different tissues, all shown in units of [ms]. It was assumed that myelin water has a shorter T_1 and T_2 than other water compartments. (D) The distribution of resonance frequencies across the voxel.

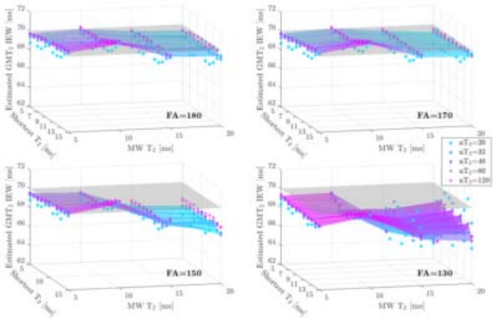

Figure 2: GMT_2 IEW estimation at different FAs, nT_2s, T_2-ranges and MW T_2s. The gray plane represents the true T_2 value of 70ms. The coloured plane corresponds to the FA estimation using 40 nT_2 values, which is the standard used in in vivo analyses. GMT_2 for IEW was well estimated, particularly at higher refocusing FAs. At lower FAs, voxels with longer MW T_2 times showed more deviation from the reference. However, variations were small, with FA=130 still estimating GMT_2 of IEW 2ms lower than the true value.

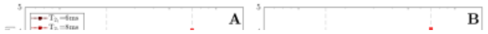

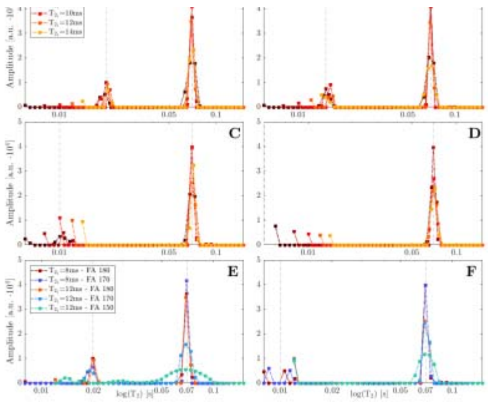

Figure 3: (A-D) T_2-distributions obtained from different T_2-ranges for varying MWT2 at optimal refocusing (FA=180) and nT_2=80. The vertical broken lines indicate the true MW and IEW T_2. The MWT_2 was reduced from A to D, corresponding to 20ms,15ms,10ms,5ms. The MWF peak was incompletely displayed when the MWT_2 is lower than allowed by the T_2-range. In this case, all signal attributed of MWT_2-component is assigned to $T_{2,1}$, thus inaccurately representing the MWT_2. Despite small variations, the $IEWT_2$ is reliably determined independent of the T_2-range. (E-F) display how lower FAs change the distribution, but preserve the GMT_2 values of the water pools if $T_{2,1}$>MWT_2.

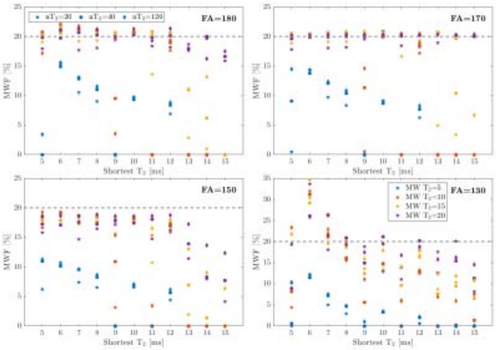

Figure 4: MWF estimation with respect to the FA, nT_2, T_2 range and MW T_2. Values related to different nT_2s are shown with different symbols and MWF values related to different MWT_2's are distinguished using different colors. For instance, MWF values assuming a MWT_2 of 5ms (blue) are consistantly underestimated even at FA=180, because the T_2-range did not account for values <5ms. In contrast, MWFs of voxels with MWT_2 of 10ms are well captured, if $T_{2,1}$ is <=10ms or just above (12ms). As the FAs reduce, the MWF is underestimated.

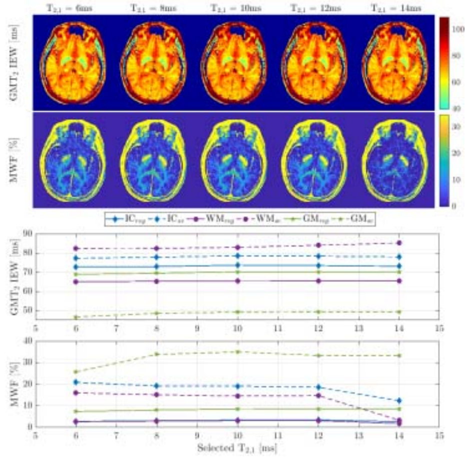

Figure 5: Impact of the selection of different T_2-ranges for *in vivo* data analysis. The resulting GMT_2 IEW maps and MWF maps are shown in the upper two rows, and the bottom rows display the average GMT_2 IEW and MWF within small regions ('_reg') of the internal capsule (IC), white matter (WM) and globus pallidus (GM) as well as single voxel ('_sv') data. Visually, the MWF improved when lowering $T_{2,1}$ from 14 to 12ms. This was reflected in the single voxel measurements, which showed an increase in MWF when lowering $T_{2,1}$. Averages over region-of-interests, however, were much less affected.